ChemistrySelect

Research Article
doi.org/10.1002/slct.202104286

Chemistry Europe
European Chemical Societies Publishing

www.chemistryselect.org

Organic & Supramolecular Chemistry

Regio- and Stereoselective Synthesis of Benzoquinolizidines

Anna Alekszi-Kaszás,[a] Klára Käfer-Beke,[b] Tamás R. Varga,[a] Attila Bényei,[c] Tibor Kovács,[d] Attila Mándi,[d] Tibor Kurtán,*[d] András Simon,[b] and Péter Nemes*[a]

Dedicated to the memory of Professor Ferenc Fülöp

An enantioselective domino Michael addition-cyclization-dehydration sequence was performed in the reaction of a 3,4-dihydroisoquinolin-1(2*H*)-ylideneethanenitrile derivative and α,β-unsaturated aldehydes using cinchona- and diphenylprolinol-type organocatalyts. The D2PM-TMS organocatalyst was found to show the best performance up to 95% enantiomeric excess. The resultant 6,7-dihydro-2*H*-pyrido[2,1-*a*]isoquinolines was reduced by catalytic hydrogenation to produce benzo[c]quinolizidines diastereoselectively with three chirality centers, the skeleton of which is a comman structural motif in alkaloids. The stereochemistry of products was studied by single crystal X-ray diffraction and solution TDDFT-ECD and DFT-VCD approaches. With the aid of VCD and ECD calculations, characteristic VCD and ECD transitions were identified, which reported the absolute configuration of the tricyclic skeleton by simple comparison regardless the different C-2 substituents.

Introduction

Activated enamines such as β-enaminonitriles,[1] β-enaminoesters[2] or nitroenamines[3] are efficient starting materials in cascade reactions with α,β-unsaturated carbonyls to prepare bridged *N*-heterocycles, indolizines, quinolizines and their benzene-anellated derivatives, containing 1,2- or 1,4-dihydropyridine moiety.[4] These products can be transformed stereoselectively by catalytic hydrogenation to various substituted bi- and tricyclic saturated derivatives.

Considering the pharmacological significance of the chiral benzoquinolizidine scaffold, the development of efficient and stereoselective synthetic routes to this class of compounds can be of strong relevance. In our previous works,[5] we demonstrated the utility of 1-cyanomethylene-tetrahydroisoquinoline (**1**) in base-, and Lewis acid-catalyzed or microwave-assisted Michael-aldol-dehydration domino sequences (Scheme 1).

We established that the KO*t*-Bu-catalyzed Michael-aldol addition gave the hemiaminal, which could be dehydrated in an acid-catalyzed reaction resulting in 6,7-dihydro-2*H*-

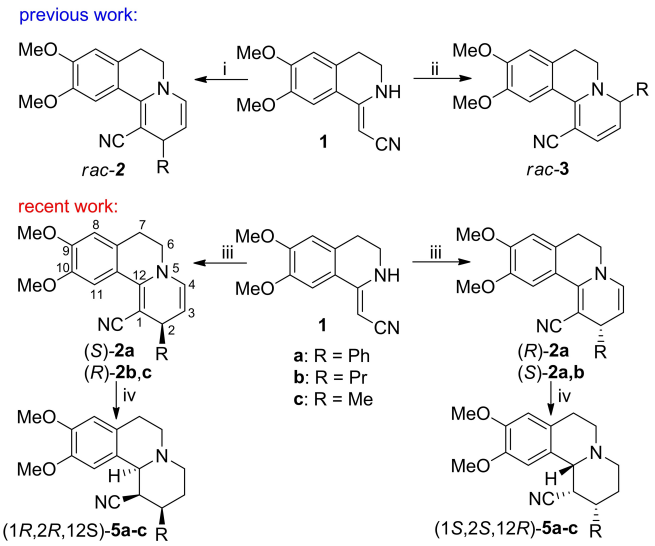

Scheme 1. i: 1. RCH=CHCHO (**4**), *t*-BuOK, 2. AcOH, EtOAc; or **4**, $CeCl_3 \times 7\ H_2O$. ii: **4**, MW. iii: **4a–c**, diphenylprolinol-TMS, ACN. iv: H_2,/PtO_2, EtOH.

[a] *A. Alekszi-Kaszás, Dr. T. R. Varga, P. Nemes*
Department of Chemistry
University of Veterinary Medicine
H-1400 Budapest, P.O.Box 2, Hungary
E-mail: nemes.peter@univet.hu
[b] *K. Käfer-Beke, Dr. A. Simon*
Department of Chemistry
University of Technology and Economics
H-1111 Budapest, Szt. Gellért tér 4, Hungary
[c] *Dr. A. Bényei*
Department of Physical Chemistry
University of Debrecen
4032 Debrecen, Hungary
[d] *T. Kovács, Dr. A. Mándi, T. Kurtán*
Department of Organic Chemistry
University of Debrecen,
P. O. Box 400, 4002 Debrecen, Hungary
E-mail: kurtan.tibor@science.unideb.hu

Supporting information for this article is available on the WWW under https://doi.org/10.1002/slct.202104286

benzo[a]quinolizines (**1**→*rac*-**2**).[5a] The $CeCl_3$ catalyzed reaction afforded directly the dehydrated product *rac*-**2**. In contrast, the microwave-assisted reactions or conventional heating gave predominantly the regioisomeric 6,7-dihydro-4*H*-benzo[a]quinolizines (**1**→*rac*-**3**) (Scheme 1). There are only a few examples in the literature for the enantioselective organocatalytic version of these domino reactions, in which the condensed 1,4-dihydropyridins were produced mostly in "head-to-tail" annulations, usually in the presence of diphenylprolinol type organocatalysts.[6]

In our recent work, we examine the regio- and stereoselectivity in the enantioselective organocatalytic reactions of the 3,4-dihydroisoquinolin-1(2*H*)-ylideneethanenitrile derivative **1** with α,β-unsaturated aldehydes to afford substituted 6,7-dihydro-2*H*-pyrido[2,1-*a*]isoquinolines containing a condensed 1,4-dihydropyridine subunit (Scheme 1; **1**→(*S*)-**2a**–**c** or (*R*)-**2a**–**c**). The products were hydrogenated to the hexahydro analogues **5a**–**c**, during which two additional chirality centers were introduced diastereoselectively. The stereochemistry of products were analyzed by the combination of single crystal X-ray diffraction, DFT-VCD and TDDFT-ECD calculations. Characteristic VCD and ECD transitions were identified, which could be used to determine the absolute configuration and they can be of help in the stereochemical study of realted tetrahydroisoquinoline alkaloids.

Results and Discussion

Regio- and enantioselective synthesis of benzoquinolizines

Cinchona-based bifunctional organocatalysts has gained much attention in enantioselective Michael additions (Figure 1),[7] which prompted us to test them in the reaction of **1** and cinnamaldehyde (**4a**) under different reaction conditions. First we performed the reaction with the QT and DQT bifunctional quinine thiourea organocatalysts, which were utilized previously in the asymmetric 1,4-addition of nitromethane to chalcone.[7j]

The reactions were carried out in CH_3CN at room temperature with 1.1 mol equivalent of cinnamaldehyde and 0.1 equivalent of the organocatalyst. The conversions were low even after several days stirring and it could not be improved by adding benzoic or trifluoracetic acid additive because of the formation of several by-products. The highest enantiomeric excess of the isolated product **2a** was 12%.

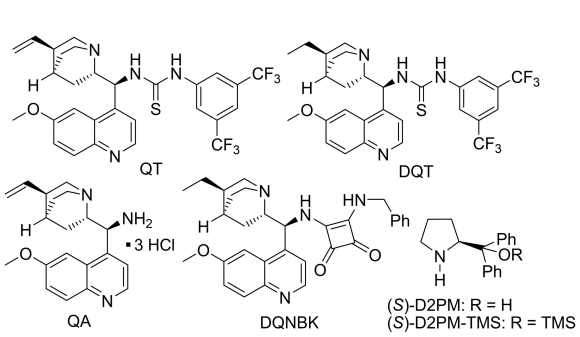

Figure 1. Structures of bifunctional quinine thiourea (QT, DQT), aminoquinine (QA), quinine-squaramide (DQNBK) and diphenylprolinol organocatalsts.

When the hydrochloric acid salt of the aminoquinine organocatalyst QA×3 HCl was used, the reaction was completed in 2 hours in acetonitrile and (*S*)-**2a** could be isolated with 58% yield and 13% ee (entry 2, Table 1). The enantiomeric excess could be increased to 29% by changing the solvent to dioxane (entry 3), while in THF and EtOAc low yields and no enantioselectivity were observed with the formation of many by-products (entry 4 and 5, Table 1).

When an equivalent amount of triethylamine (TEA) was used with QA×3 HCl to generate the free amine base, the regioselectivity of the reaction changed to head-to-head annulation and the racemic 6,7-dihydro-4*H*-benzo[a]quinolizine derivative *rac*-**3a** was obtained with 55% yield in CH_3CN and with 61% in CH_2Cl_2 after 24 and 36 hours, respectively (entry 6 and 7). HMBC and NOE correlations were utilized to distinguish the (*S*)-**2a** and *rac*-**3a** regioisomers. The 2-H methine proton gave a HMBC correlation with the C-1 in (*S*)-**2a**, whereas H-4/H-6 NOE correlation was observed in *rac*-**3**.[5b]

The lack of enantioselectivity suggested that either the imine, formed in the reaction of the aldehyde and the QA, or the aldehyde reacted initially with the β carbon of the enamine moiety to form an achiral azatriene intermediate. An analogue of this intermediate could be isolated previously as a precursor of the 4*H*-regioisomer.[5d,e] The subsequent 1,6-electrocyclization provided necessarily the racemate of the 4*H*-regioisomer *rac*-**3**. (Scheme 2).

When using quinine-squaramide organocatalyst DQNBK, the reaction took place only in the presence of equimolar TFA additive and it afforded (*S*)-**2a** with moderate yield (45%) and low enantiomeric excess (48%) (entry 8, Table 1). By using QA and DQNBK organocatalysts in the presence of an acid, the formation of a by-product was always observed up to 30% yield, the HPLC/MS analysis of which showed that it is a mixture of two compounds in 65:35% ratio with the molar mass of 688 D. This suggested that a dimerization of the initial 4*H*-benzo[a]quinolizine derivative **2a** may have occurred resulting in heterodimers. Due the overlapping NMR signals of the

Table 1. Reactions of **1** and cinnamaldehyde using aminoquinine organocatalysts.

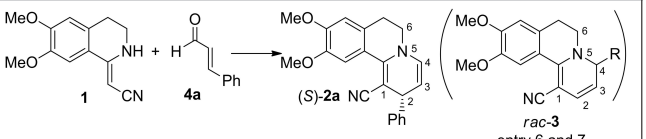

Entry	Catalyst	Solvent	Time (h)	Product (%)	ee (%)
1	QA·3HCl	MeCN	1.5	(*S*)-**2a** (53)	13
2	QA·3HCl	MeCN	2	(*S*)-**2a** (58)	18
3	QA·3HCl	dioxane	0.5	(*S*)-**2a** (55)	29
4	QA·3HCl	THF	1.5	(*S*)-**2a** (<10)	0
5	QA·3HCl	EtOAc	1.5	(*S*)-**2a** (<10)	0
6	QA+TEA	MeCN	24	*rac*-**3** (55)	0
7	QA+TEA	CH_2Cl_2	36	*rac*-**3** (61)	0
8	DQNBK +TFA	MeCN	8	(*S*)-**2a** (45)	48

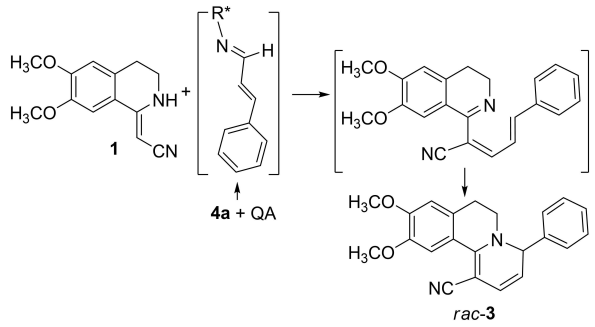

Scheme 2. Proposed mechanism for the formation of *rac*-**3**.

isomeric mixture, the exact structural elucidation of these dimers was not performed.

The poor performance of the cinchona-type catalysts prompted us to turn to the D2PM and D2PM-TMS diphenylprolinol organocatalyst (Figure 1). When reacting **1** with cinnamaldehyde in the presence of (*S*)-DP2 M, the reaction was complete in 72 hours and **2a** was isolated with 65% yield but no enantioselectivity could be detected (entry 1, Table 2). However, with (*S*)-DP2 M-TMS, 85% enantiomeric excess and 48% yield could be achieved at room temperature (entry 2). The reactions were carried out repeatedly in different solvents at room and reflux temperature with and without acidic additives. The main product was always (*R*)-**2a** containing the 1,4 dihydropyridine moiety. A small amount of the regioisomeric *rac*-**3** could be observed in all the reactions, which could be isolated with 3–10% yield as a racemate. By heating the reaction to reflux temperature, the reaction rate could be increased considerably but somewhat lower enantiomeric excess values were measured (entry 3). The use TFA as an additive led to the formation of many by-products but benzoic acid accelerated the reaction without changing the enantiomeric excess (entry 4). Increasing the amount of the organocatalyst to 30% molar equivalent did not improve the enantioselectivity or the yield (entry 5 and 6). The solvents dichloromethane (DCM) and ethyl acetate were also tested (entry 7–11) and 95% enantiomeric excess could be achieved with 58% yield in ethyl acetate (entry 10). The organocatalytic processes were carried out both with (*R*)- and (*S*)-D2PM-TMS to obtain obtain both enantiomers

Table 2. Enantioselective organocatalytic preparation of (*R*)-**2a** in the presence of diphenylprolinol-type catalysts.

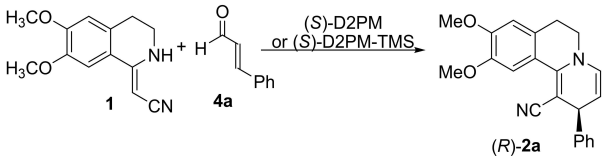

Entry	Cat. (amount %)	Temp.(°C)	Solvent	Reaction time (h)	Yield (%)	ee %[a]
1	A (10)	25	ACN	72	65	0
2	B (10)	25	ACN	24	48	85
3	B (10)	80	ACN	2	64	68
4	B (10)[b]	25	ACN	4	58	81
5	B (30)[b]	25	ACN	24	62	86
6	B (30)[b]	80	ACN	2	58	76
7	B (10)[b]	25	DCM	72	53	88
8	B (20)[b]	25	DCM	72	68	92
9	B (10)[b]	25	DCM	4	69	82
10	B (10)[b]	25	EtOAc	72	58	95
11	B (10)[b]	25	EtOAc	5	56	91

isolated yield.b) 10 mol% benzoic acid is used as an acidic additive.

The organocatalytic reaction was also performed with the reagents 2-hexenal and crotonaldehyde by using the conditions of entry 10, and (*R*)-**2b** and (*R*)-**2c** were obtained with 58% and 64% enantiomeric excess, respectively. The base-line separation of their enantiomers was not successful on normal phase Chiralcel columns and on a reversed phase Chiral-AGP column. Thus the enantiomeric excess was determined by the HPLC separation of their hydrogenated derivative (*vide infra*).

In order to demonstrate the potential of the enantioselective organocatalytic process, the optically active 2*H*-benzoquinolizidines **2a–c** were reduced by catalytic hydrogenation using PtO_2 catalyst in EtOH (Scheme 1). The resultant tricyclic substituted 1,3,4,6,7,11b-hexahydro-2*H*-pyrido[2,1-*a*]isoquinoline skeleton is a common structural unit in chiral tetrahydroisoquinoline alkaloids such as ipecac alkaloids, the stereochemistry of which was often studied by electronic circular dichroism analysis.[8] Both enantiomers of **2a–c** were hydrogenated, which provided diastereoselectively the (1*R*,2*R*,12*S*)-**5a–c** from (*R*)-**2a–c** and (1*S*,2*S*,12*R*)-**5a–c** from (*S*)-**2a–c** (Scheme 1). The (1*R**,2*R**,12*S**) relative configurations of **5a** and **5b** were determined by single crystal X-ray diffraction analysis, which also provided unambiguously the (1*S*,2*S*,12*R*) absolute one for **5a** obtained from (*S*)-**2a** with 0.03 value of the Flack parameter (Figure 2a).

Since the sample of **5b** contained the two enantiomers in 79:21 ratio, the Flack parameter was 0.2 and absolute configuration (AC) was also confirmed by chiroptical methods (*vide infra*). The chiral non-racemic **5a–c** derivatives were used to test the applicability of electronic (ECD) and vibrational circular dichroism (VCD) aided by TDDFT and DFT calculations to determine their absolute configuration. The VCD approach has been emerged as a powerful chiroptical technique to distinguish more than two stereoisomers[9] and determine the AC of natural products.[10] The ECD and VCD analysis of **5a–c**

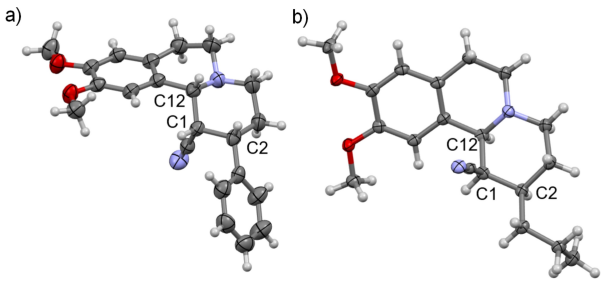

Figure 2. a) ORTEP structure (50% probability) of (1*S*,2*S*,12*R*)-**5a** obtained in the catalytic hydrogenation of (*R*)-**2a**. b) ORTEP structure (50% probability) of (1*R*,2*R*,12*S*)-**5b** obtained in the catalytic hydrogenation of (*R*)-**2b**.

my serve as a reference how to determine the stereochemistry of related tetrahydroisoquinoline alkaloids with chiroptical approaches.

The enantiomers of **5b** showed decent mirror-image experimental ECD and VCD spectra (Figure 3), which were utilized for the solution TDDFT-ECD and DFT-VCD protocols.[11] The initial Merck Molecular Force Field (MMFF) conformational search of the arbitrarily chosen (1*R*,2*R*,12*S*)-**5a** resulted in 112 initial conformer clusters in a 21 kJ/mol energy window. The further ωB97X/TZVP PCM/MeCN and B3LYP/TZVP PCM/$CHCl_3$ re-optimizations of these yielded 13 low-energy conformers over 1% Boltzmann population (Figure S22). In the low-energy solution conformers of (1*R*,2*R*,12*S*)-**5a**, the heteroring adopted *M*-helicity with axial orientation of 12-H and the C–1 nitrile group and equatorial one of the C–2 propyl (Figure 4). The conformational flexibility of the molecule consisted in the rotation of the C–9 and C–10 methoxy and the C–2 *n*-propyl groups, while the other parts were rigid. When examining the computed VCD or ECD spectra of the individual 13 conformers, we found that the computed VCD spectra of all the B3LYP conformers were very similar regardless the different orientation of the methoxy or propyl groups. In contrast, two different conformational ensembles were identified among the ωB97X conformers of the ECD calculation, which differed mainly in the orientation of the methoxy groups but exhibited significantly different computed ECD curves (Figure 5). Group A contained conformers A–D, F, H, J, K, M with a total population of 85.6%; while group B had conformers E, G, I, L with a total population of 5.9%. The Boltzmann-weighted computed ECD and VCD spectra of (1*R*,2*R*,12*S*)-**5b** reproduced very well the experimental spectra of (−)-**5b**, prepared from (*R*)-**2b** (Figure 3), which was in accordance with the result of the X-ray analysis. The good agreement of the experimental and computed VCD curves would allow excluding the other possible (1*S*,2*R*,12*R*)-**5a** stereoisomer of the catalytic hydrogenation even without determining the relative configuration.

The VD spectra of (1*R*,2*R*,12*S*)-**5b** and (1*S*,2*S*,12*R*)-**5b** were compared with those of (1*R*,2*R*,12*S*)-**5a** and (1*S*,2*S*,12*R*)-**5c** to identify characteristic VCD transitions, which did not change significantly by altering the C–3 substituent and thus allow the determination of AC by simple comparison of the VCD spectra (Figure 6).

Interestingly, the VCD curve of (1*R*,2*R*,12*S*)-**5a** showed all the major VCD transitions with the same sign as that of (1*R*,2*R*,12*S*)-**5b** in the wavelength range of 1100–1450 cm^{-1}, on the basis of which the AC could be assigned unambiguously without further calculations. In (1*R*,2*R*,12*S*)-**5a**, the alternating signs of the nearby intense 1269, 1257, 1246 cm^{-1} transitions, the positive signs of the 1221 and 1207 cm^{-1} transitions and the intense positive 1144 and 1109 cm^{-1} bands of (1*R*,2*R*,12*S*)-**5b** were reproduced well and they showed the same VCD

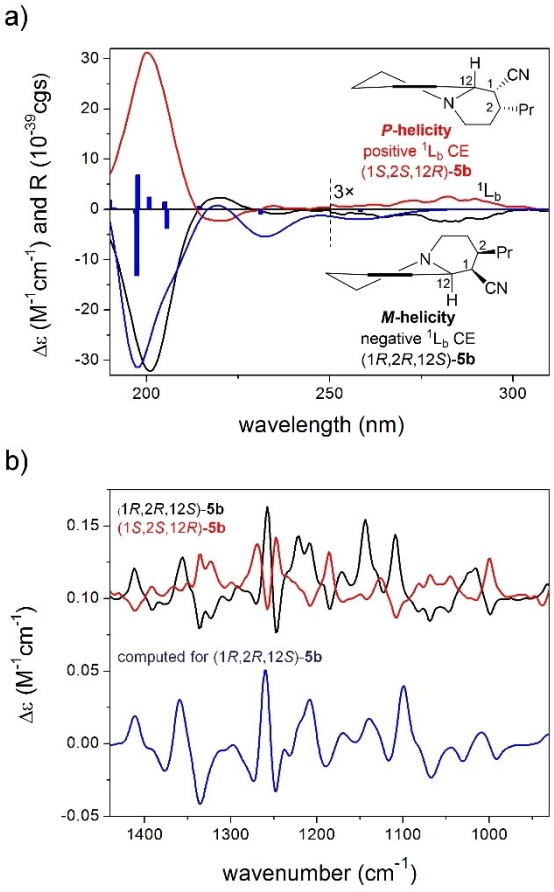

Figure 3. Mirror-image experimental ECD (a) and VCD (b) spectra of (1*R*,2*R*,12*S*)-**5b** (black) and (1*S*,2*S*,12*R*)-**5b** (red) compared with the computed ECD and VCD spectra of (1*R*,2*R*,12*S*)-**5b** (blue). For better visibility of the characteristic ^1L_b ECD transition, the experimental ECD spectra were multiplied by 3 above 250 nm. Blue bars in the ECD figure represent the computed rotatory strength values of the lowest-energy conformer.

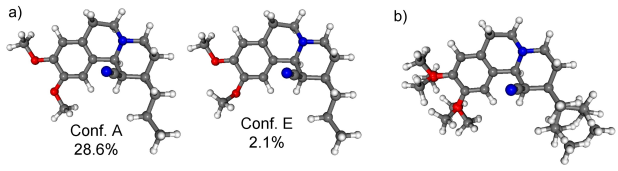

Figure 4. a) Low-energy representative ωB97X/TZVP PCM/MeCN conformers of (1*R*,2*R*,12*S*)-**5b** producing different ECD spectra b) Overlapped structures of the thirteen low-energy conformers of (1*R*,2*R*,12*S*)-**5b** obtained at the B3LYP/TZVP PCM/$CHCl_3$ level of theory utilized for the VCD calculations.

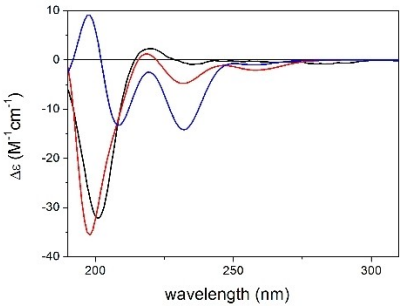

Figure 5. Experimental ECD spectrum of (1*R*,2*R*,12*S*)-**5b** (black) compared with the computed ECD spectra of conformers A (red) and E (blue) representing the two distinct conformational ensembles, group A and B of (1*R*,2*R*,12*S*)-**5b**.

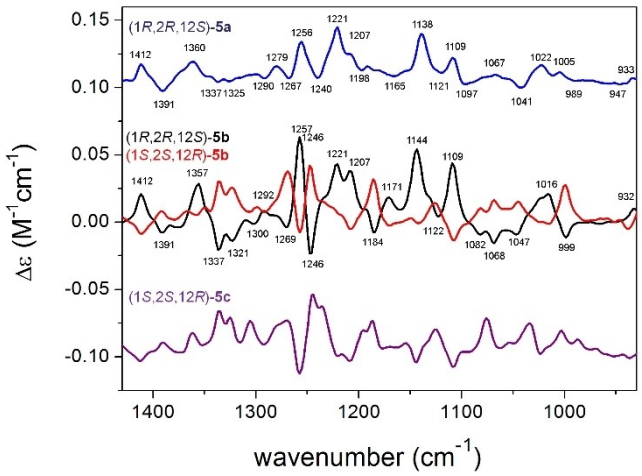

Figure 6. Experimental VCD spectra of (1*R*,2*R*,12*S*)-**5 a** (blue) and (1*S*,2*S*,12*R*)-**5 c** (purple) compared to (1*R*,2*R*,12*S*)-**5 b** (AKA-45) (black) and (1*S*,2*S*,12*R*)-**5 b** (red).

patterns (Figure 6). All these VCD transitions are associated with C–H deformation, C–C and C–N stretching and deformation vibrations of the quinolizidine skeleton and thus they can be utilized to report the AC of C–2, C–3 and C–12 regardless the type of the C–2 substituent. Moreover, the characteristic VCD transitions were not sensitive to the conformational differences arising from different orientations of the methoxy groups or the C–2 substituent. The VCD transitions of (1*S*,2*S*,12*R*)-**5 c** resembled those of (1*S*,2*S*,12*R*)-**5 b** in the wavelength range of 1100–1450 cm^{-1} allowing the configurational assignment on the basis of simple comparison.

The comparison of the experimental ECD spectra of (1*S*,2*S*,12*R*)-**5 a**, -**5 b** and (1*R*,2*R*,12*S*)-**5 a**, -**5 b** revealed that intense ECD band at about 200 nm and the ^1L_b band above 260 nm report also equally well the AC of the quinolizidine skeleton regardless the presence of absence of the C–2 phenyl group (Figure 7). The stereoisomers of **5 a**–**c** contain a 1,2,3,4-tetrahydroisoquinoline chromophore, the helicity and hence the absolute configuration of which was correlated with the sign of the high-wavelength ^1L_b band Cotton effect (CE) by a helicity rule.[12]

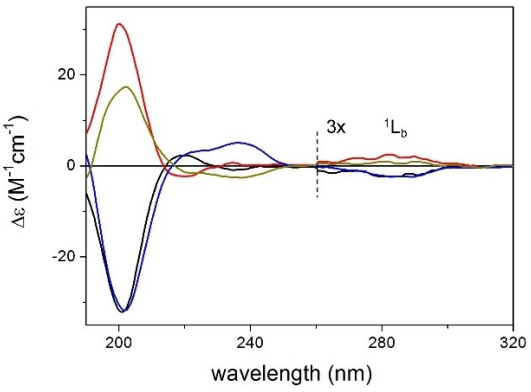

Figure 7. Experimental ECD spectra of (1*R*,2*R*,12*S*)-**5 a** (blue), (1*S*,2*S*,12*R*)-**5 a** (olive) compared to (1*R*,2*R*,12*S*)-**5 b** (black) and (1*S*,2*S*,12*R*)-**5 b** (red). For the better visualization of the ^1L_b region, the transitions above 260 nm were multiplied by 3.

According to this rule, the *P*-helicity of the condensed chiral heteroring is manifested in a positive ^1L_b CE, while the *M*-helicity in a negative one (Figure 3a).[12a] The C–9 and C–10 methoxy substituent of the benzene ring and the isolated weak nitrile chromophore are not expected to change this helicity rule. Our ECD calculations confirmed that the tetrahydroisoquinoline helicity rule worked well for the configurational assignment of the stereoisomers of **5 a**–**c**. In (1*R*,2*R*,12*S*)-**5 b**, the heteroring adopted *M*-helicity in order to fix the preferred equatorial orientation of the C–12–C–1 bond as confirmed by the geometry of the X-ray diffraction analysis and DFT conformers (Figure 2b, 3a, 4). The *M*-helicity of (1*R*,2*R*,12*S*)-**5 b** was reflected in a negative broad ^1L_b CE with vibronic fine structure, and this correlation did not change for (1*R*,2*R*,12*S*)-**5 b** when there was an additional remote phenyl chromophore C–2. Interestingly, the ECD spectrum of the octahydro-protoberberine alkaloids, alangiifoliumine A, showed the same ECD pattern for the low-wavelength CEs as that of (1*R*,2*R*,12*S*)-**5 b**, since the chirality of the heteroring (C–12 in **5 b** and C–13a in alangiifoliumine A) is expected to have the largest contribution to the ECD[12a]. However, the characteristic weak high-wavelength ^1L_b CE was completely overlooked and it was not even recorded.

Conclusion

Cinchona-based and diphenylprolinol-type organocatalysts were tested in the domino Michael addition-cyclization-dehydration reactions of a 3,4-dihydroisoquinolin-1(2*H*)-ylideneethanenitrile derivative to afford substituted 6,7-dihydro-2*H*-pyrido[2,1-*a*]isoquinolines containing a condensed 1,4-dihydropyridine subunit. In the domino reaction, the D2PM-TMS organocatalyst was proved to achieve enantiomeric excess and yield up to 95% and 69%, respectively. The products of domino reactions were hydrogenated in the presence of PtO_2 catalyst to produce optically active benzo[c]quinolizidine derivatives diastereoselectively with three contiguous chirality centers. Their stereochemistry was investigated by two single crystal X-ray geometries in the solid state and by DFT-VCD and TDDFT-ECD calculations in solutions. The VCD calculations identified characteristic VCD transitions associated with the vibrations of the quinolizidine skeleton, which could be used for comparison regardless the type of the C–2 substituent and they were not sensitive to the different orientation of the methoxy or C–2 propyl groups in the solution conformers. The comparison of the ECD spectra assisted by TDDFT-ECD calculations showed that the tetrahydroisoquinoline helicity rule correlating the high-wavelength ^1L_b CE with the helicity of the heteroring and the AC can be used to determine the AC, which can aid the configurational assignment of related tetrahydroisoquinoline alkaloids. The scope of the organocatalytic enantioselective reaction is to be tested in further works.

Deposition numbers

Deposition Numbers 2115501 (for **5 a**) and 2115449 (for **5 b**) contain the supplementary crystallographic data for this paper. These data are provided free of charge by the joint Cambridge Crystallographic Data Center and Fachinformationszentrum Karlsruhe http://www.ccdc.cam.ac.uk/structures.

Supporting Information Summary

Experimental details, characterization, ^{1}H, ^{13}C NMR of the compounds prepared, the data of the single crystal measurements, and the experimental ECD spectra are presented in the Supporting Information.

Acknowledgements

The PhD scholarship from Szent István University to A. Alekszi-Kaszás is gratefully acknowledged. The research work was supported by the National Research, Development and Innovation Office (K138672 FK134653).

Conflict of Interest

The authors declare no conflict of interest.

Data Availability Statement

The data that support the findings of this study are available in the supplementary material of this article.

Keywords: benzoquinolizidines · cascade reactions · enantioselective organocatalysis · Michael additions · TDDFT-ECD · DFT-VCD

[1] a) A. W. Erian, *Chem. Rev.* **1993**, *93*, 1991; b) Y. Cheng, Z. T. Huang, M.-X. Wang, *Current Org. Chem.* **2004**, *8*, 325.
[2] a) C. Altug, M. C. Elliott, B. M. Kariuki, T. Rorstad, M. Zaal, Y. Dueruest, *Org. Biomol. Chem.* **2010**, *8*, 4978; b) K. Paulvannan, J. R. Stille, *J. Org. Chem.* **1994**, *59*, 1613; c) J. H. Kim, S. G. Lee, H. J. Shin, *J. Org. Chem.* **2012**. *77*, 1560; d) C. Altug, M. C. Elliott, Y. Dueruest, *Tetrahedron Lett.* **2009**, *50*, 7392.
[3] a) F. Felluga, G. Pitacco, C. Visintin, E. Valentin, *Helv. Chim. Acta* **1997**, *80*, 1457; b) I. S. Hutchinson, S. A. Matlin, A. Mete, *Tetrahedron Lett.* **2001**, *42*, 1773; c) M. V. Pilipecz, T. R. Varga, P. Scheiber, Z. Mucsi, A. Fŕvre-Mourgues, S. Boros, L. Balázs, G. Tóth, P. Nemes, *Tetrahedron* **2012**, *68*, 5547; d) M. V. Pilipecz, Z. Mucsi, P. Nemes, P. Scheiber, *Heterocycles* **2007**, *71*, 1919; e) A. Avadhani, P. Iniyavan, A. Acharya, V. Gautam, S. Chakrabarti, H. Ila, *ACS Omega* **2019**, *4*, 17910.
[4] V. K. Sharmaa, S. K. Singh, *RSC Adv.* **2017**, *7*, 2682 and references therein.
[5] a) P. Nemes, B. Balázs, G. Tóth, P. Scheiber, *Synlett* **1999**, *2*. 222; b) P. Nemes, Z. Vincze, B. Balázs, G. Tóth, P. Scheiber, *Synlett* **2003**, *2*. 250; c) Z. Vincze, P. Nemes, B. Balázs, G. Tóth, P. Scheiber, *Synlett* **2004**, 1023; d) Z. Vincze, Z. Mucsi, P. Scheiber, P. Nemes, *Eur. J. Org. Chem.* **2008**, *6*, 1092; e) Z. Vincze, P. Nemes, *Tetrahedron* **2011**, *67*, 3380; f) Z. Vincze, P. Nemes, *Tetrahedron* **2013**, *69*, 6269.
[6] a) M.-X. Zhao, M.-X. Wang, Z.-T. Huang, *Tetrahedron* **2002**, *58*, 1309; b) G. S. Buchanan, D. Huifang, R. P. Hsung, A. I. Gerasyuto, C. M. Scheinebeck, *Org. Lett.* **2011**, *13*, 4402; c) X. Wu, L. Nie, H. Fang, J. Chen, W. Cao, G. V. Zhao, *Eur. J. Org. Chem.* **2011**, *9*, 6755; d) A. Noole, M. Borissova, M. Lopp, T. J. Kanger, *J. Org. Chem.* **2011**, *76*, 1538; e) Y. Lou, Y. Xu, Z. Chai, X. Shao, G. Zhao, Z. Li, *Tetrahedron* **2015**, *71*, 6651.
[7] a) M. H. Freund, S. B. Tsogoeva, *Synlett* **2011**, *4*, 503; b) B. List, P. Pojarliev, H. J. Martin, *J. Org. Lett.* **2001**, *3*, 2423; c) S. J. Wagh, G. R. Dhage, *Synlett* **2017**, *28*. 1353. K. Vanlaldinpuia, P. B. Lalthanpuii, *Science Vision* **2016**, *16*, 123 and references therein; d) Y.-C. Chen *Synlett* **2008**, *13*, 1919. S. Mukherjee, J. W. Yang, S. Hoffmann, B. List, *Chem. Rev.* **2007**, *107*, 5471; e) B. Vakulya, S. Varga, T. Soós, *Org. Chem.* **2008**, *73*, 3475; f) A. Bacsó, M. Szigeti, S. Varga, T. Soós, *Synthesis* **2017**, *49*, 429; g) B. Kótai, G. Kardos, A. Hamza, V. Farkas, I. Pápai, T. Soós, *Chem. Eur. J.* **2014**, *20*, 5631; h) B. Vakulya, S. Varga, A. Csámpai, T. Soós, *Org. Lett.* **2005**, *7*, (10), 1967; i) S. Varga, G. Jakab, L. Drahos, T. Holczbauer, M. Czugler, T. Soós, *Org. Lett.* **2011**, *13*, 5416; j) B. Vakilya, S. Varga, A. Csámpai, T. Soós, *Org. Lett.* **2005**, *7*, 1967–1969.
[8] a) Y.-S. Cai, C. Wang, C. Tian, W.-T. Sun, L. Chen, D. Xiao, S. Zhou, G. Qiu, J. Yu, K. Zhu, S.-P. Yang, *J. Nat. Prod* **2019**, *82*, 2645–2652; b) A. Itoh, Y. Ikuta, Y. Baba, T. Tanahashi, N. Nagakura, *Phytochemistry* **1999**, *52* 1169–1176; c) A. Itoh, Y. Ikuta, T. Tanahashi, N. Nagakura, *J. Nat. Prod.* **2000**, *63*, 723–725.
[9] W.-Y. Ding, Y.-M. Yan, X.-H Meng, A. L. Nafie, T. Xu, K. R. Dukor, H.-B. Qin, X.-Y. Cheng, *Org. Lett.* **2020**, *22*, 5726-5730.
[10] a) K. H. Hopmann, J. Šebestík, J. Novotná, W. Stensen, M. Urbanová, J. Svenson, J. S. Svendsen, P. Bouř, K. J. Ruud, *J. Org. Chem.* **2012**, *77*, 858-869; b) P. L. Polavarapu, E. Santoro, *Nat. Prod. Rep.* **2020**, *37*, 1661-1699; c) M. Kato, M. A. S. Hammam, T. Taniguchi, Y. Suga, K. Monde, *Org. Lett.* **2016**, *18*, 768–771; d) M. A. J. Koenis, C. S. Chibueze, W. J. Buma, M. A. Jinks, S. M. Goldup, V. P. Nicu, L. Visscher, W. Buma, *J. Chem. Sci.* **2020**, *11*, 8469–8475.
[11] a) S. Superchi, P. Scafato, M. Górecki, G. Pescitelli, *Curr. Med. Chem.* **2018**, *25*, 287–320; b) A. Mándi, T. Kurtán, *Nat. Prod. Rep.* **2019**, *36*, 889–918.
[12] a) G. Snatzke, P. C. Ho, *Tetrahedron* **1971**, *27*, 3645–3653; b) S. Hagishita, K. Kuriyama, *Bull. Chem. Soc. Jpn.* **1982**, *55*, 3216–3224; c) J. Toda, S. Matsumoto, T. Saitoh, T. Sano, *Chem. Pharm. Bull.* **2000**, *48*, 91–98.

Submitted: December 2, 2021
Accepted: January 4, 2022